Facile Electron Transfer to CO2 During Adsorption at the Metal | Solution Interface

Gauthier, Joseph A.; Fields, Meredith; Bajdich, Michal; Chen, Leanne D; Sandberg, Robert B.; Chan, Karen; Nørskov, Jens K.

Published in:
Journal of Physical Chemistry C

Link to article, DOI:
10.1021/acs.jpcc.9b10205

Publication date:
2019

Document Version
Peer reviewed version

Facile Electron Transfer to CO_2 during Adsorption at the Metal | Solution Interface

Joseph A. Gauthier,[b] Meredith Fields,[b] Michal Bajdich,[a] Leanne D. Chen,[b,†] Robert B. Sandberg,[b] Karen Chan,[c] and Jens K. Nørskov[,c]*

[a]SUNCAT Center for Interface Science and Catalysis, SLAC National Accelerator Laboratory, Menlo Park, California, 94025, United States

[b]SUNCAT Center for Interface Science and Catalysis, Department of Chemical Engineering, Stanford University, Stanford, California 94305, United States.

[c]Department of Physics, Technical University of Denmark, 2800 Kongens Lyngby, Denmark

[†]Present Address: Division of Chemistry and Chemical Engineering, California Institute of Technology, Pasadena, California 91125, United States

***Corresponding Author:** Jens K. Nørskov: jkno@dtu.dk

Abstract

*We estimate the rate of electron transfer to CO_2 at the Au (211)|water interface during adsorption in an electrochemical environment under reducing potentials. Based on density functional theory calculations at the generalized gradient approximation and hybrid levels of theory, we find electron transfer to adsorbed *CO_2 to be very facile. This high rate of transfer is estimated by the energy distribution of the adsorbate-induced density of states as well as from the interaction between diabatic states representing neutral and negatively charged CO_2. Up to 0.62 electrons are transferred to CO_2, and this charge adiabatically increases with the bending angle to a lower limit of 137°. We conclude that this rate of electron transfer is extremely fast compared to the timescale of the nuclear degrees of freedom, that is, the adsorption process.*

Introduction

Electrochemical CO_2 reduction is studied intensively since it can provide a route to sustainable production of fuels.[1] Among candidates tested over many decades of research, a handful of transition and coinage metal catalysts have shown mentionable activity. For CO_2 reduction to CO, Au has the highest activity, producing CO with a current density of 1mA/cm^2 at a potential below −0.4V under neutral conditions.[2–7] More reduced products are found at considerably lower potentials over Cu catalysts,[2,8,9] and with substantially lower Faradaic yields on other transition metals.[6] While product distributions and trends in catalytic activity are relatively well-documented, mechanistic questions, beginning with the first step, remain contentious.

The first step in CO_2 reduction is the adsorption of CO_2. It has been suggested that an electron transfer to the adsorbing CO_2 molecule dictates the overall rate of reduction to CO.[4,10,11] The main argument in favor of rate-limiting electron transfer is that product current densities on these metals depend only on the absolute electrode potential and not on pH. A lack of pH dependence suggests that the rate-limiting step(s) does not involve a proton transfer. However, the absence of pH dependence on the rate leaves room for interpretation. For example, it has been shown that both permanent and induced dipole moments of adsorbate molecules interact strongly with the fields at the electrode interface.[12–14] The interfacial field strength depends on the absolute or Standard Hydrogen Electrode (SHE) potential scale and can significantly influence the binding energy of intermediates, such as CO_2, through this dipole-field interaction. In the case that CO_2 adsorption is rate limiting, the overall reaction rate could still show a dependence on the absolute electrode potential, even with facile electron transfer.

Adsorbed CO_2 is observed both computationally and experimentally to be negatively charged in a bent geometry.[15–17] Therefore, adsorption is indeed associated with some electron transfer to the adsorbate. The reduction potential of CO_2 in aqueous solution is on the order of −1.8 V vs SHE,[18] which is considerably more negative than the potential where CO_2 is reduced over Ag and Au.[19] Therefore, the electron transfer must take place in the vicinity of the catalyst surface, where the surface interacts sufficiently strongly with the CO_2 molecule to stabilize the negative molecular ion.[10] The fundamental question that we investigate here is whether electron transfer in this adsorption process can be rate determining.

Theoretical and Computational Details

CO_2 adsorption over Au (211) surface at negative potentials was modeled by including a Na^+ ion solvated in a water layer above the (3x3) supercell surface, with 10 Å of vacuum separating periodic images. Dipole corrections[20] were applied during optimizations to decouple the electrostatic interaction between periodic images in the *z*-direction. The bottom two layers of each slab were constrained at the bulk lattice constant during adsorbate and water layer optimizations while the top layer of metal atoms was allowed to relax until all forces fell below a threshold of 0.05 eV/Å. The total system is shown in Figure 1. The starting point was a set of DFT-GGA calculations optimized with the Vienna Ab-Initio Simulation Package,[21–24] (VASP) using projector-augmented wave (PAW) pseudopotentials[25,26] to describe the core electrons, with valence electrons expanded as

plane-waves up to a cutoff of 500 eV. At the GGA level of DFT, the RPBE exchange-correlation functional[27] was used. The hybrid-DFT calculations employed the range-separated, screened HSE06 functional.[28,29] A (4×4×1) Monkhorst-Pack *k*-point sampling was used for all calculations except the calculation of the projeted density of states (PDOS), for which a more dense sampling of (8x8x1) with a Gaussian smearing of 0.2 eV was used.[30] An initial guess for the solvent, ion, and adsorbate configuration was provided through minima hopping.[31] From these minima, initial and final states with CO_2 close to and far from the surface were calculated by reoptimizing each structure with the CO_2 adsorbate. Only the lowest energy structures were selected for final analysis.

A climbing-image nudged elastic band (NEB)[32,33] calculation was performed to generate the lowest energy path from solvated to adsorbed CO_2. To determine the energetics of each diabatic path (linear and bent), the optimized geometry of the (linear and bent, respectively) CO_2 molecule was applied to each image along the converged adsorption path. In other words, the position of the C atom was the same between the two diabatic curves for each image, and only the O=C=O angle was constrained to match the optimized bent or linear bond angle. Single-point energy evaluations were performed on top of these geometries to generate the diabatic curves in Figure 4. The resulting structures and energies are also available online at catalysis-hub.org repository.[34,35]

Results and Discussion

In order to better understand the rate of CO_2 adsorption during electro-reduction and the role of electron transfer, we have calculated the potential energy diagram and electronic structure of adsorbing CO_2 over a stepped Au (211) surface at negative potentials (vs SHE) using density functional theory (DFT). We present the electronically adiabatic reaction pathway as well as pathways for two cases where the O=C=O angle is fixed in both a linear and a bent configuration corresponding to the neutral and negative ions, respectively. We then calculate a measure of the rate of electron transfer in the region of interest using both generalized gradient approximation (GGA)-DFT and hybrid-DFT, the latter including both exact exchange and non-local correlation effects. We conclude that the rate of electron transfer is extremely fast compared to the time scale of the adsorption process. It is therefore unlikely that electron transfer is rate limiting for this reaction.

In our calculation of CO_2 adsorption on a negatively charged Au (211) electrode surface, we model the outer Helmholtz plane by a water bilayer including a solvated Na ion as in shown in **Figure 1**. The total system is electroneutral, and hence, excess electrons in the surface are exactly countered by Na^+ ions to form an electrochemical double layer at which the adsorption occurs. Given that Au has a potential of zero charge of ~0.2eV[36], a standard capacitance of 20μF/cm^2 would give a potential of ~-0.7V vs SHE for the system considered. The Supporting Information (SI) and an online database[35] provides all the corresponding structures and energies.

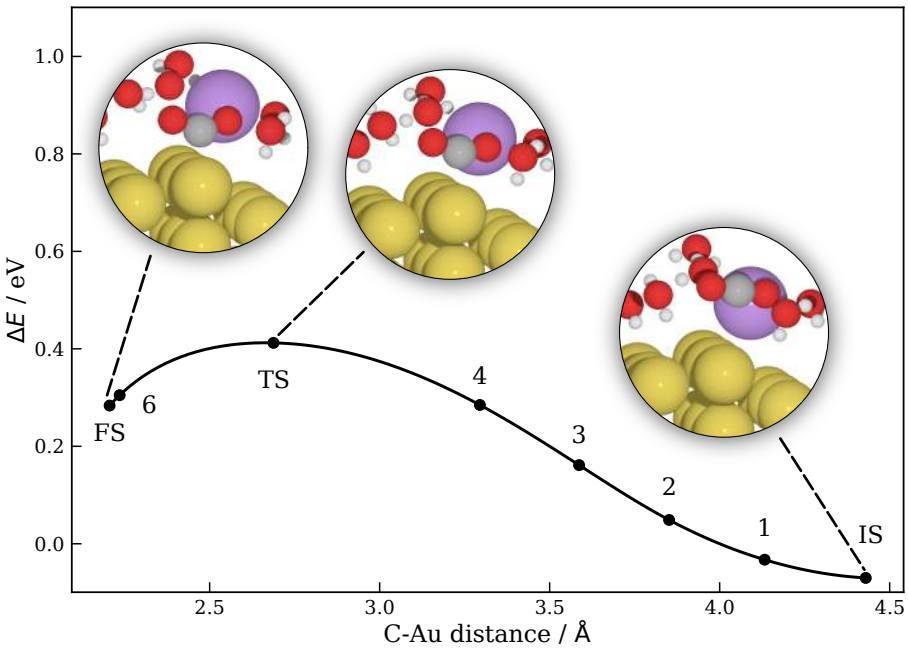

Figure 1: Adiabatic Pathway for CO_2 adsorption (from right to left) on Au (211) surface in the presence of a Na^+ ion solvated in a water bilayer. The calculated potential energy path is as function of the horizontal distance, d_z, of CO_2 molecule from the top of the surface. Energies are referenced to gas phase CO_2 molecule and clean surface with the solvated ion. The insets highlight the geometries of initial (IS), transition (TS) and final (FS) states. The carbon atom is shown in gray, oxygen and hydrogen atoms shown as red and white and Na^+ ion as large purple sphere. For all structures, please refer to the SI, or to an available online database.[35]

First, we perform a calculation which is adiabatic in the electronic and CO_2 nuclear degrees of freedom along the reaction pathway. **Figure 1** shows the resulting potential energy diagram calculated using the RPBE exchange correlation functional[27] (see also Computational Details). The energy, plotted on the *y*-axis, shows that the CO_2 adsorption is slightly uphill in energy at the considered surface charge density. The energies in this plot are referenced to a gas phase CO_2 molecule and a clean, solvated surface. Each inset represents a particular snapshot of the CO_2 structure along the path. It can be seen that the solvated CO_2 molecule in the outer Helmholtz plane bends along the reaction pathway, indicative of partial transfer of an electron to the molecule.[37] We note that endothermic adsorption does not preclude further reaction. Instead, it indicates that the activation energy for the total process will include the positive reaction energy of this first step. Since the coverage of adsorbed CO_2 will be first order in the CO_2 activity in solution (or CO_2 pressure), the total rate will also be first order. We note that this finding is also supported across a range of experiments.[4,5,10]

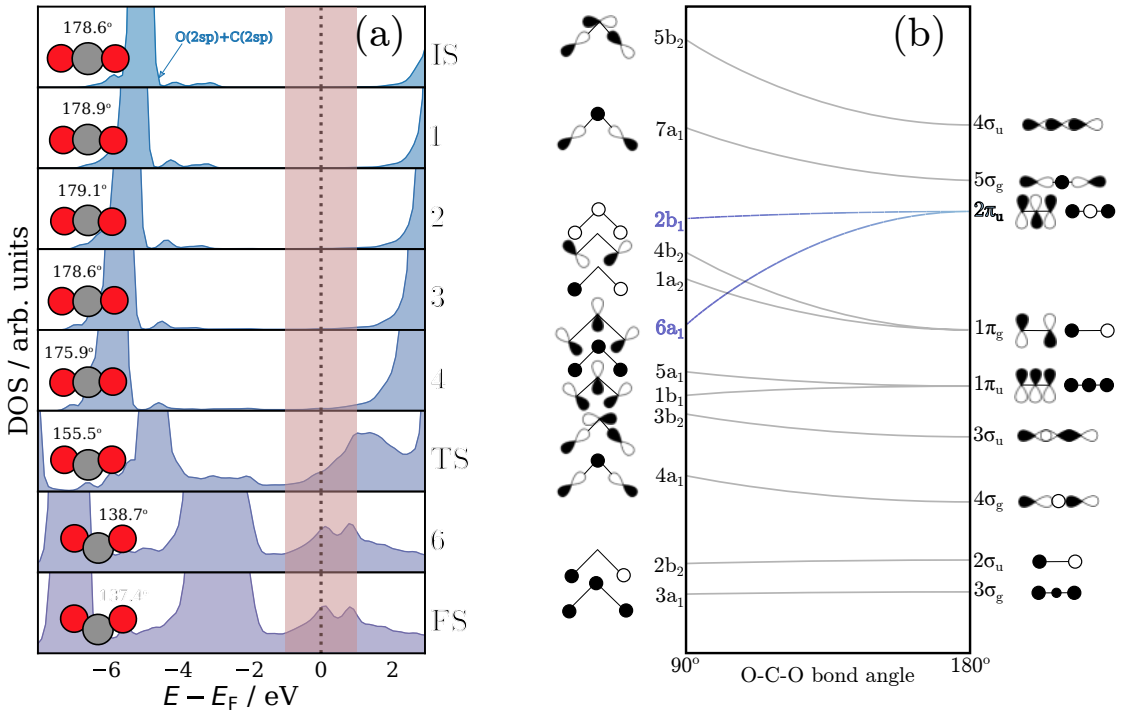

Figure 2: (a) Evolution of the projected density of states (PDOS) along the adsorption pathway, where the s and p states of the two oxygen atoms and one carbon atom of CO_2 are shown. The CO_2 bending angle is indicated in the insets. We highlight (in light red) the observed 1 eV broadening at the Fermi level as the molecule approaches the surface. (b) Walsh diagram for carbon dioxide, showing the splitting of π states as the molecule transitions from the linear to bent configuration. Adapted from ref. [37]. Reproduced with permission. Copyright Elsevier 1996.

Now we address the question of whether it is a good approximation to assume that the electronic degrees of freedom are adiabatic—that is, whether the electron transfer is rate-limiting. We approach this problem in two ways. First, we consider the evolution in the projected density of states (PDOS) for the CO_2 molecule carbon and oxygen atoms (2*s* and 2*p*) along the adiabatic pathway, shown in **Figure 2 (a)**. It can be seen that all bonding CO_2 states are filled and the antibonding states[37] are well above the Fermi level when the molecule is far away from the surface. As the molecule approaches the surface and starts to adopt the bent geometry, the degenerate antibonding states start to split. The lower edge of the states moves down through the Fermi level along the pathway, indicating an electron transfer to form a partially charged adsorbed CO_2 anion. This is further illustrated by the Walsh diagram for the CO_2 molecule, as shown in Figure 2 (b), reproduced with permission from ref. [37].

It can be seen that all molecular states are broadened into resonances. This is observed generally for adsorption of atoms and molecules on metal surfaces.[38–41] One way of looking at this is that the electrons can hop between the adsorbate states and continuum of metal states with which they interact. The electrons therefore have a finite lifetime in the adsorbate states and thus a corresponding uncertainty in the energy. In the Newns-Anderson model of chemisorption,[38–40] the energy width of the adsorbate states is given by $\Delta = \sum_k |V_{ak}|^2 \delta(\epsilon_a - \epsilon_k)$, where V_{ak} is the coupling matrix element between metal state k and adsorbate state a, and ϵ_k and ϵ_a are the corresponding orbital energies. It can be seen that $\frac{2\pi}{\hbar}\Delta$ is simply the Fermi Golden Rule expression of the rate of electron transfer. From **Figure 2**, it can be seen that the width of the CO_2 states is of the order 1 eV (highlighted in

light red near the Fermi level) corresponding to a rate of electron transfer of the order 10^{15} s^{-1}.

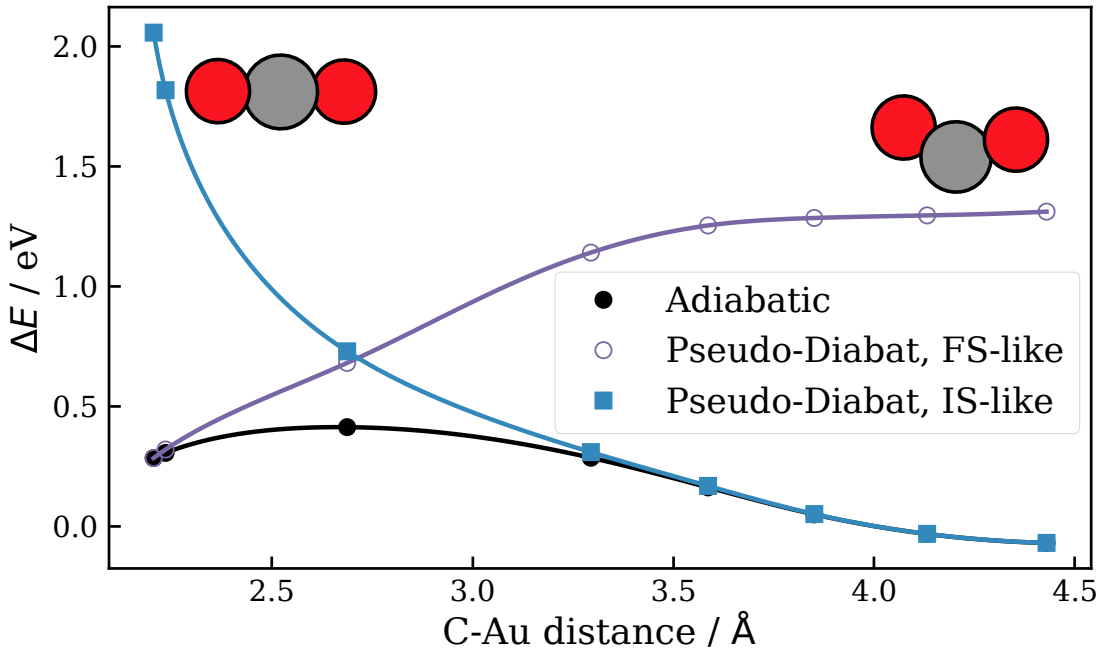

Figure 3: Diabatic potential energy curves for CO_2 adsorption on an Au (211) surface. Solid squares represent the path where CO_2 is constrained in a linear geometry while approaching the surface. Open circles represent the path where CO_2 is constrained in a bent (negatively charged) geometry while approaching the surface.

An alternative viewpoint, illustrated in **Figure 3**, is to consider the adsorption event as a transition between two pseudo-diabatic potential energy curves. In one of these curves, the O=C=O angle is kept fixed at the value 180˚, corresponding to the initial, neutral state of the CO_2 molecule, labeled as IS′. In the other curve, the angle is kept fixed at 137.4˚, corresponding to the final, anionic state, FS. According to a Bader analysis, the bent geometry carries a negative charge (from –0.27 to –0.62 e), while the linear geometry stays essentially neutral (see SI **Figure S1**). The two curves therefore also represent two charge states of the CO_2 molecule. Far from the surface, in the first outer Helmholtz plane, the neutral state is favored over the anionic state by about 1 eV. However, the energies of the two states of CO_2 cross at a distance of ~2.6 Å from the surface near the transition state. Eventually, the charged and bent molecular state becomes energetically favorable close to FS, while the neutral state is highly disfavored. The adiabatic path is also indicated in **Figure 3** in black circles.

At the point where the linear CO_2 configuration is no longer favored energetically, the metal surface may transfer an electron to the CO_2 molecule, allowing the anti-bonding state to be occupied. The lowest energy path for this process, and the ability of Au (211) to transfer an electron into the CO_2 molecule and stabilize the bent CO_2 configuration, is represented by the adiabatic path, which can be viewed as the bonding state resulting from the interaction between the two diabatic states. It can be seen from the energy difference between the diabatic crossing point and the adiabatic barrier that the strength of the

coupling at the crossing point is on the order of several tenths of an eV, reinforcing the result from above that the coupling is strong enough such that the transfer rate is very high.

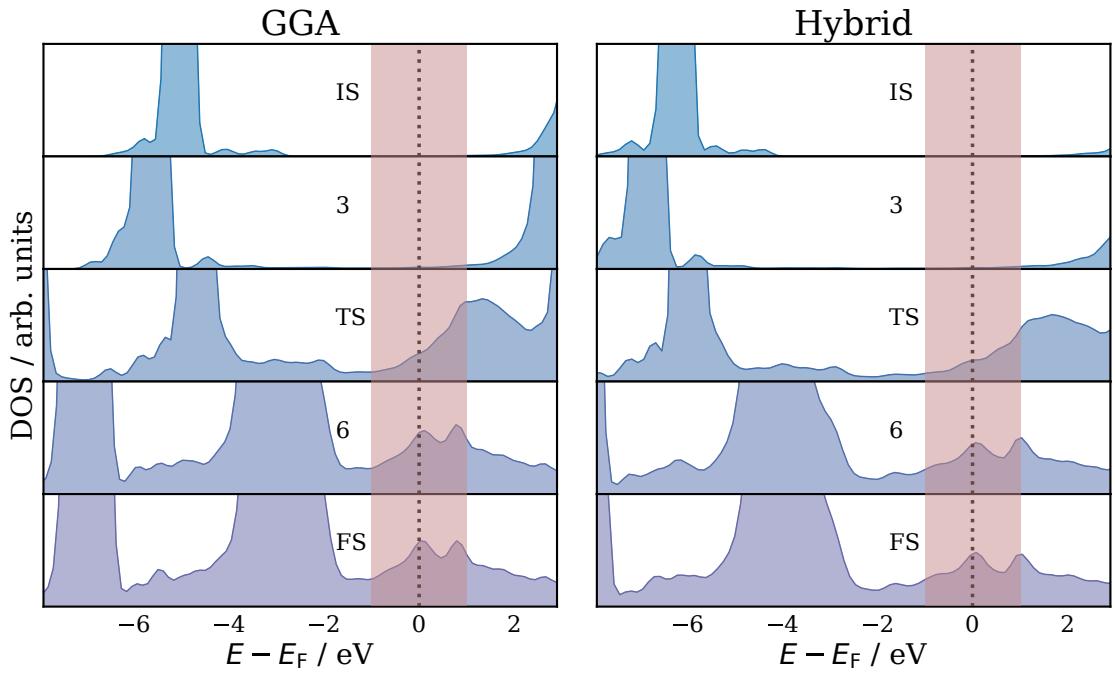

Figure 4: Comparison of the RPBE (left) and HSE06 (right) evolutions of projected density of states analogous to **Figure 2**. Only the selected images from **Figure 1** are shown.

In order to verify that the results are not limited to semi-local DFT, we also calculate the adsorbate spectra using the screened range-separated hybrid HSE06 functional (see also Computational Details). The resulting spectra calculated using the RPBE and HSE06 functionals[28,29] are compared in **Figure 4** for selected points along the adiabatic pathway. As expected, the HOMO-LUMO gaps for the molecular states are increased for HSE06, compared to the semi-local DFT results. However, the broadening of the bands (~1 eV), which is the primary quantity of interest in this study, has not changed significantly particularly at the Fermi level.

Conclusions

We conclude from the results shown here that electron transfer is unlikely to be rate-determining in CO_2 adsorption. We suggest that this result holds for any electrochemical adsorption process occurring close to a metal surface where the overlap of molecular and metal states is large enough to help stabilize the charged adsorbate. This scenario is in stark contrast to outer-sphere electron-transfer reactions in solution.[42] The main difference between the two scenarios are twofold. First, the electron transfer is over a long distance and the reductant is not directly involved in stabilizing the transition state. Second, as a metal surface has electrons available for all energies below the Fermi level (down to the bottom of the conduction band), this substantially relaxes the requirement for an exact energy alignment between the donor and acceptor levels. Of course, these current findings would not be transferable to insulating or semi-conducting surfaces that do not have a continous density of states below the Fermi level. Typically, insulators can only be

of interest as electrocatalysts if they are thin enough that electrons can be transported through, either by electron hopping or tunneling. In such cases, electron transport can easily become rate limiting.[43]

The current results raise the question: why is the rate of CO_2 reduction found to be independent of pH for a fixed absolute potential? Adsorbed CO_2 has a significant dipole moment of –0.49 eÅ (SI **Figure S2**), which would be stabilized by the fields exerted by ions at the electrochemical double-layer.[44] Since these fields depend on absolute potential, so would the field-stabilized CO_2 binding energy. If CO_2 binding is the limiting step, the overall rate would also have no pH dependence. We believe that the above implications remain valid for a broader class of adsorption processes, despite the simplified model of the electrochemical interface employed in this work.

Acknowledgments

This material is based upon work performed by the Joint Center for Artificial Photosynthesis, a DOE Energy Innovation Hub, supported through the Office of Science of the U.S. Department of Energy under Award Number DE-SC0004993. This work uses resources of the National Energy Research Scientific Computing Center, a DOE Office of Science User Facility, supported by the Office of Science of the U.S. Department of Energy under Contract No. DE-AC02-05CH11231. M. F. also acknowledges NSF for a Graduate Fellowship. K. C. and J. K. N. also acknowledge support from Research Grant 9455 from VILLUM FONDEN.

References

(1) Lu, Q.; Jiao, F. Electrochemical CO2reduction: Electrocatalyst, Reaction Mechanism, and Process Engineering. *Nano Energy* **2016**, *29*, 439–456.

(2) Hori, Y.; Takahashi, R.; Yoshinami, Y.; Murata, A. Electrochemical Reduction of CO at a Copper Electrode. *J. Phys. Chem. B* **1997**, *101* (36), 7075–7081.

(3) Jitaru, M.; Lowy, D. A.; Toma, M.; Toma, B. C.; Oniciu, L. Electrochemical Reduction of Carbon Dioxide on Flat Metallic Cathodes. *J. Appl. Electrochem.* **1997**, *27* (8), 875–889.

(4) Wuttig, A.; Yaguchi, M.; Motobayashi, K.; Osawa, M.; Surendranath, Y. Inhibited Proton Transfer Enhances Au-Catalyzed CO2-to-Fuels Selectivity. *Proc. Natl. Acad. Sci.* **2016**, *113* (32), E4585–E4593.

(5) Dunwell, M.; Lu, Q.; Heyes, J. M.; Rosen, J.; Chen, J. G.; Yan, Y.; Jiao, F.; Xu, B. The Central Role of Bicarbonate in the Electrochemical Re- Duction of Carbon Dioxide on Gold. *J. Am. Chem. Soc.* **2017**.

(6) Hori, Y. Electrochemical CO2 Reduction on Metal Electrodes - Modern Aspects of Electrochemistry; Vayenas, C. G., White, R. E., Gamboa-Aldeco, M. E., Eds.; Springer New York: New York, NY, 2008; pp 89–189.

(7) Kuhl, K. P.; Hatsukade, T.; Cave, E. R.; Abram, D. N.; Kibsgaard, J.; Jaramillo, T. F. Electrocatalytic Conversion of Carbon Dioxide to Methane and Methanol on Transition Metal Surfaces. *J. Am. Chem. Soc.* **2014**, *136* (40), 14107–14113.

(8) Kyriacou, G.; Anagnostopoulos, A. Electroreduction of CO2 on Differently Prepared Copper Electrodes: The Influence of Electrode Treatment on the Current

Efficiences. *J. Electroanal. Chem.* **1992**, *322* (1–2), 233–246.
(9) Momose, Y.; Sato, K.; Ohno, O. Electrochemical Reduction of CO2 at Copper Electrodes and Its Relationship to the Metal Surface Characteristics. *Surf. Interface Anal.* **2002**, *34* (1), 615–618.
(10) Hori, Y.; Murata, A.; Kikuchi, K.; Suzuki, S. Electrochemical Reduction of Carbon Dioxides to Carbon Monoxide at a Gold Electrode in Aqueous Potassium Hydrogen Carbonate. *J. Chem. Soc. Chem. Commun.* **1987**, No. 10, 728–729.
(11) Varela, A. S.; Kroschel, M.; Leonard, N. D.; Ju, W.; Steinberg, J.; Bagger, A.; Rossmeisl, J.; Strasser, P. PH Effects on the Selectivity of the Electrocatalytic CO 2 Reduction on Graphene-Embedded Fe–N–C Motifs: Bridging Concepts between Molecular Homogeneous and Solid-State Heterogeneous Catalysis. *ACS Energy Lett.* **2018**, *3* (4), 812–817.
(12) Deshlahra, P.; Conway, J.; Wolf, E. E.; Schneider, W. F. Influence of Dipole–Dipole Interactions on Coverage-Dependent Adsorption: CO and NO on Pt(111). *Langmuir* **2012**, *28* (22), 8408–8417.
(13) Zhang, P.; Cai, J.; Chen, Y.; Tang, Z.; Chen, D.; Yang, J.; Wu, D.; Ren, B.; Tian, Z. Potential-Dependent Chemisorption of Carbon Monoxide at a Gold Core - Platinum Shell Nanoparticle Electrode : A Combined Study by Electrochemical in Situ Surface-Enhanced Raman Spectroscopy and Density Functional Theory. *J. Phys. Chem.* **2009**, *113* (40), 17518–17526.
(14) Nørskov, J. K.; Holloway, S.; Lang, N. D. Microscopic Model for the Poisoning and Promotion of Adsorption Rates by Electronegative and Electropositive Atoms. *Surf. Sci.* **1984**, *137* (1), 65–78.
(15) Wang, S.-G.; Cao, D.-B.; Li, Y.-W.; Wang, J.; Jiao, H. Chemisorption of CO2 on Nickel Surfaces. *J. Phys. Chem. B* **2005**, *109* (40), 18956–18963.
(16) Liu, C.; Cundari, T. R.; Wilson, A. K. CO 2 Reduction on Transition Metal (Fe, Co, Ni, and Cu) Surfaces: In Comparison with Homogeneous Catalysis. *J. Phys. Chem. C* **2012**, *116* (9), 5681–5688.
(17) Dzade, N. Y.; Roldan, A.; De Leeuw, N. H. Activation and Dissociation of CO<inf>2</Inf> on the (001), (011), and (111) Surfaces of Mackinawite (FeS): A Dispersion-Corrected DFT Study. *J. Chem. Phys.* **2015**, *143* (9).
(18) Koppenol, W. H.; Rush, J. D. Reduction Potential of the Carbon Dioxide/Carbon Dioxide Radical Anion: A Comparison with Other C1 Radicals. *J. Phys. Chem.* **1987**, *91* (16), 4429–4430.
(19) Zhao, S.; Jin, R.; Jin, R. Opportunities and Challenges in CO2 Reduction by Gold- and Silver-Based Electrocatalysts: From Bulk Metals to Nanoparticles and Atomically Precise Nanoclusters. *ACS Energy Lett.* **2018**, *3* (2), 452–462.
(20) Bengtsson, L. Dipole Correction for Surface Supercell Calculations. *Phys. Rev. B* **1999**, *59* (19), 12301–12304.
(21) Kresse, G.; Furthmüller, J. Efficient Iterative Schemes for *Ab Initio* Total-Energy Calculations Using a Plane-Wave Basis Set. *Phys. Rev. B* **1996**, *54* (16), 11169–11186.
(22) Kresse, G.; Hafner, J. Ab Initio Molecular Dynamics for Liquid Metals. *47* (1), 558–561.
(23) Kresse, G.; Furthmüller, J. Efficiency of Ab-Initio Total Energy Calculations for Metals and Semiconductors Using a Plane-Wave Basis Set. *6* (1), 15–50.

(24) Kresse, G. From Ultrasoft Pseudopotentials to the Projector Augmented-Wave Method. *Phys. Rev. B* **1999**, *59* (3), 1758–1775.
(25) Blöchl, P. E. Projector Augmented-Wave Method. *50* (24), 17953–17979.
(26) Kresse, G.; Joubert, D. From Ultrasoft Pseudopotentials to the Projector Augmented-Wave Method. *59* (3), 1758–1775.
(27) Hammer, B.; Hansen, L. B.; Nørskov, J. K. Improved Adsorption Energetics within Density-Functional Theory Using Revised Perdew-Burke-Ernzerhof Functionals. *Phys. Rev. B* **1999**, *59* (11), 7413–7421.
(28) Heyd, J.; Scuseria, G. E.; Ernzerhof, M. Hybrid Functionals Based on a Screened Coulomb Potential. *J. Chem. Phys.* **2003**, *118* (18), 8207–8215.
(29) Heyd, J.; Scuseria, G. E.; Ernzerhof, M. Erratum: "Hybrid Functionals Based on a Screened Coulomb Potential" [J. Chem. Phys. 118, 8207 (2003)]. *J. Chem. Phys.* **2006**, *124* (21), 219906.
(30) Monkhorst, H. J.; Pack, J. D. Special Points for Brillouin-Zone Integrations. *13* (12), 5188–5192.
(31) Goedecker, S. Minima Hopping: An Efficient Search Method for the Global Minimum of the Potential Energy Surface of Complex Molecular Systems. *J. Chem. Phys.* **2004**, *120* (21), 9911–9917.
(32) Henkelman, G.; Uberuaga, B. P.; Jónsson, H. A Climbing Image Nudged Elastic Band Method for Finding Saddle Points and Minimum Energy Paths. *J. Chem. Phys.* **2000**, *113* (22), 9901–9904.
(33) Henkelman, G.; Jónsson, H. Improved Tangent Estimate in the Nudged Elastic Band Method for Finding Minimum Energy Paths and Saddle Points. *J. Chem. Phys.* **2000**, *113* (22), 9978–9985.
(34) Winther, K. T.; Hoffmann, M. J.; Boes, J. R.; Mamun, O.; Bajdich, M.; Bligaard, T. Catalysis-Hub.Org, an Open Electronic Structure Database for Surface Reactions. *Sci. Data* **2019**, *6* (1), 75.
(35) Computational data available at https://www.catalysis-hub.org/publications/GauthierFacile2019.
(36) Trasatti, S.; Lust, E. The Potential of Zero Charge. *Mod. Asp. Electrochem.* **1999**, *329* (33), 1–215.
(37) Freund, H.-J.; Roberts, M. W. Surface Chemistry of Carbon Dioxide. *Surf. Sci. Rep.* **1996**, *25* (8), 225–273.
(38) Anderson, P. W. Localized Magnetic States in Metals. *Phys. Rev.* **1961**, *124* (1), 41–53.
(39) Edwards, D. M.; Newns, D. M. Electron Interaction in the Band Theory of Chemisorption. *Phys. Lett. A* **1967**, *24* (4), 236–237.
(40) Muscat, J. P.; Newns, D. M. Chemisorption on Metals. *Prog. Surf. Sci.* **1978**, *9* (1), 1–43.
(41) Nørskov, J. K.; Studt, F.; Abild-Pedersen, F.; Bligaard, T. *Fundamental Concepts in Heterogeneous Catalysis*; John Wiley & Sons, Inc: Hoboken, NJ, USA, 2014.
(42) Ramaswamy, N.; Mukerjee, S. Influence of Inner- and Outer-Sphere Electron Transfer Mechanisms during Electrocatalysis of Oxygen Reduction in Alkaline Media. *J. Phys. Chem. C* **2011**, *115* (36), 18015–18026.
(43) Viswanathan, V.; Pickrahn, K. L.; Luntz, A. C.; Bent, S. F.; Nørskov, J. K. Nanoscale Limitations in Metal Oxide Electrocatalysts for Oxygen Evolution.

Nano Lett. **2014**, *14* (10), 5853–5857.
(44) Chen, L. D.; Urushihara, M.; Chan, K.; Nørskov, J. K. Electric Field Effects in Electrochemical CO $_2$ Reduction. *ACS Catal.* **2016**, *6* (10), 7133–7139.

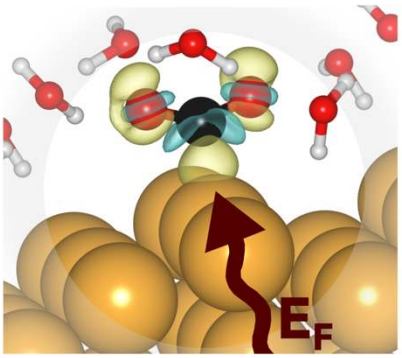

Facile electron transfer

Figure: Table Of Contents